*Supplementary Information*

# The Reversible Piezochromic Luminescence Behavior of Carbon Dots under a Cycle of Loading/Unloading Pressure

Lele Liu,[a] Menghui Ma,[a] Lei Jiang,[a] Zijian Li,[b] Vladimir Yu. Osipov,[a,c] Ting Geng,[d] Guanjun Xiao[d]* and Hong Bi[b]*

[a]School of Chemistry and Chemical Engineering, Anhui University, Hefei, 230601, China.

[b]School of Materials Science and Engineering, Anhui University, Hefei, 230601, China.

[c]International Research and Educational Center for Physics of Nanostructures, ITMO University, 197101 St. Petersburg, Russia.

[d]State Key Laboratory of Superhard Materials, College of Physics, Jilin University, Changchun 130012, China

## 1.Experimental details

**1.1 Materials.** All chemicals used are commercially available without further treatment. D-Aspartic acid (98%), ethylenediamine and commercial ethanol (99.7%) were obtained from local supplies and used as received. All water used during the experiment was ultrapure water from the microporous system (GZY-P10-B).

**1.2 Synthesis of H-CDs and M-CDs.** H-CDs sample was prepared by a hydrothermal method with aspartic acid and ethylenediamine as raw materials. Typically, 1.8 g of aspartic acid and 2 mL of ethylenediamine were added to ultrapure water, sealed in a Teflon-lined autoclave and then treated in the autoclave at 200 °C for 8 h. The powder sample of yellow color was thereafter collected and filtered after autoclave cooling down to room temperature. Subsequently, the filtrate was dialyzed using a dialysis membrane (MWCO 500-1000, Solarbio) for three days and then freeze-dried to obtain black powder. Finally, H-CDs powder was collected for further investigation. In its turn the M-CDs sample was synthesized by microwave-assisted thermal decomposition method. Similarly, 1.8 g of aspartic acid and 2 mL of ethylenediamine were dissolved in 10 mL ultrapure water, stirred vigorously until the solution became clear and transparent, and then the obtained solution was heated in a 500 W microwave oven at 100°C for 5 min. After a similar purification process to the above-mentioned one including filtration, dialysis and freeze-drying, a certain amount of M-CDs powder was collected for further structural, elemental and optical investigations.

**1.3 Characterization.** The sample's morphology and structure were examined by using transmission electron microscopy (TEM, JEM-2100, JEOL, Tokyo, Japan). Powder X-ray diffraction (XRD) analyses were carried out on SmartLab 9KW (Rigaku, Japan) with Cu Kα radiation (wavelength 1.5418 Å). A fluorescence spectrophotometer (F-4500, Hitachi, Japan) and a UV-1800PC spectrophotometer were used to study PL behavior and ultraviolet-visible (UV-vis) absorbance (Shimadzu, Japan) of samples, respectively. A calibrated integrating sphere using a HORIBA FLSP920 system (Horiba, Japan) was used to assess the absolute fluorescence quantum yield (QY). A Thermo

Nicolet NEXUS-870 ESP FT-IR/FT-NIR spectrometer (SpectraLab Scientific Inc.) was used to collect Fourier-transform infrared (FT-IR) absorption spectra. Near Edge X-ray Absorption Fine Structure (NEXAFS) analyses were carried out at the Catalysis and Surface Science Endstation at the BL11U beamline in the National Synchrotron Radiation Laboratory (NSRL) in Hefei, China. X-ray photoelectron spectroscopy (XPS) studies were performed on a commercial spectrophotometer (ESCALAB 250, Thermo Fisher Scientific, USA). Raman spectra were recorded using a laser confocal micro-Raman spectroscopy (InVia-Reflex, Renishaw, London, Britain).

**1.4 Piezochromic luminescence test of H-CDs and M-CDs.** In the experiment, a T301 steel gasket was pre-indented to 45 μm in thickness by DAC apparatus with a platen diameter of 400 μm. After removing the gasket from the press, a hole of approximately 130 μm in diameter was drilled in the pit using a laser drilling machine. Subsequently, ultrasonication was performed on the gasket with the holes drilled to remove any impurities. Under a microscope, the gasket with a hole was repositioned to its original location based on the markings made during pre-pressing, ensuring perfect alignment with the lower diamond platen. At this time, the lower diamond platen and stainless-steel sheet formed an open sample chamber. The previous work can effectively prevent leakage after the pressure transfer medium is introduced later. Using a sharpened needle sanded with sandpaper, the sample and ruby were carefully placed into the pit formed by the lower diamond platen and gasket under a microscope. An appropriate amount of silicone oil was drawn up using a capillary tube and dropped into the sample chamber, which was quickly sealed with the upper diamond platen, completing the sample loading process. In high pressure experiment, silicone oil, a colorless and transparent liquid, provided hydrostatic pressure for H-CDs and M-CDs under high pressure without any detectable effect on their behavior. All of the measurements were performed at room temperature. A brief schematic diagram of the pressure device is shown in Fig. S1.

## 2. Figures S1-S11 and Tables S1-S3

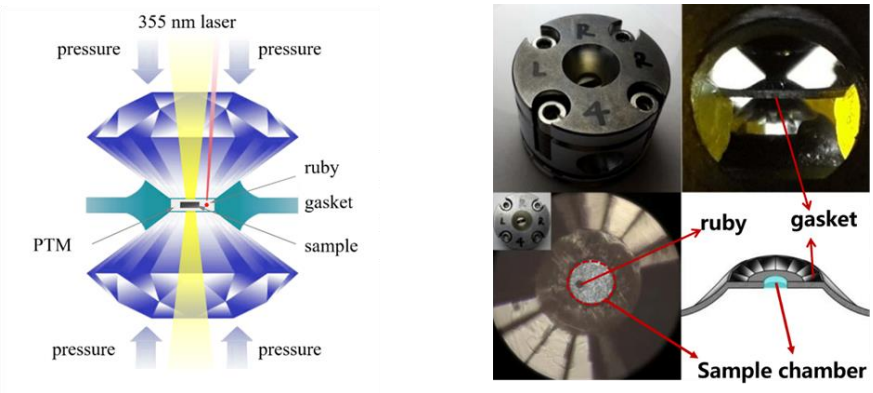


**Fig. S1** Schematic diagram and physical image of the used high-pressure device.

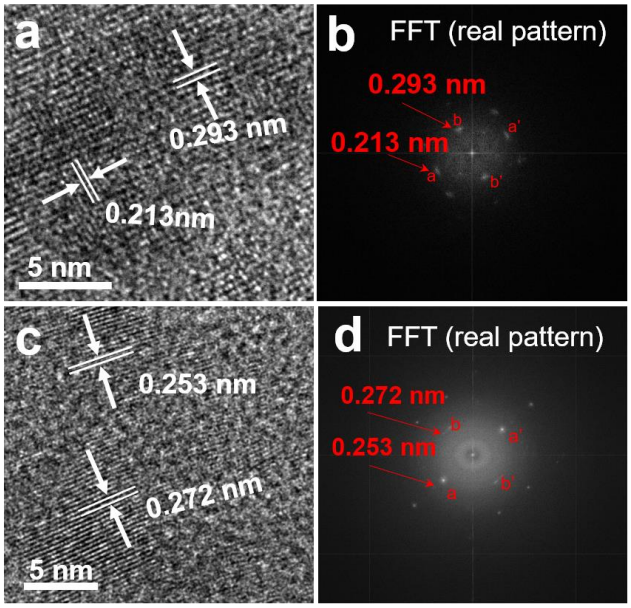


**Fig. S2** (a) HRTEM image and (b) the FFT pattern of H-CDs before compression. (c) HRTEM image and (d) the FFT pattern of M-CDs before compression.

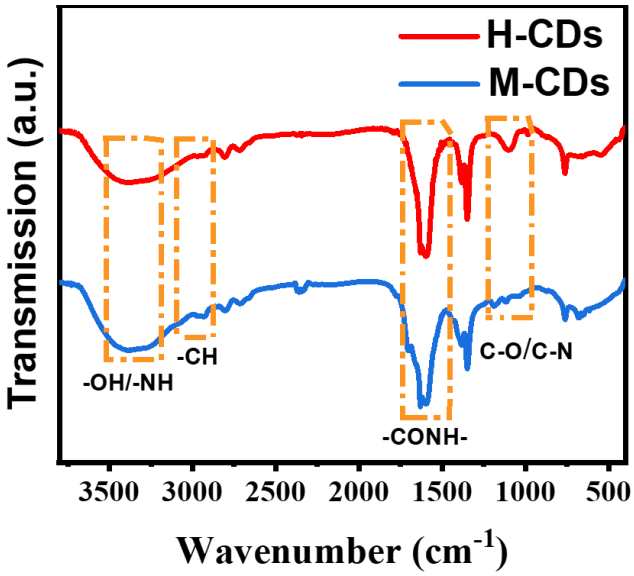


**Fig. S3** FT-IR transmission spectra of H-CDs and M-CDs. The plateau in each spectrum in the region of 1900-2000 $cm^{-1}$ corresponds to maximum transmission (≤ 100%) and almost zero absorption. The spectra are shifted along the vertical axis for easy reading.

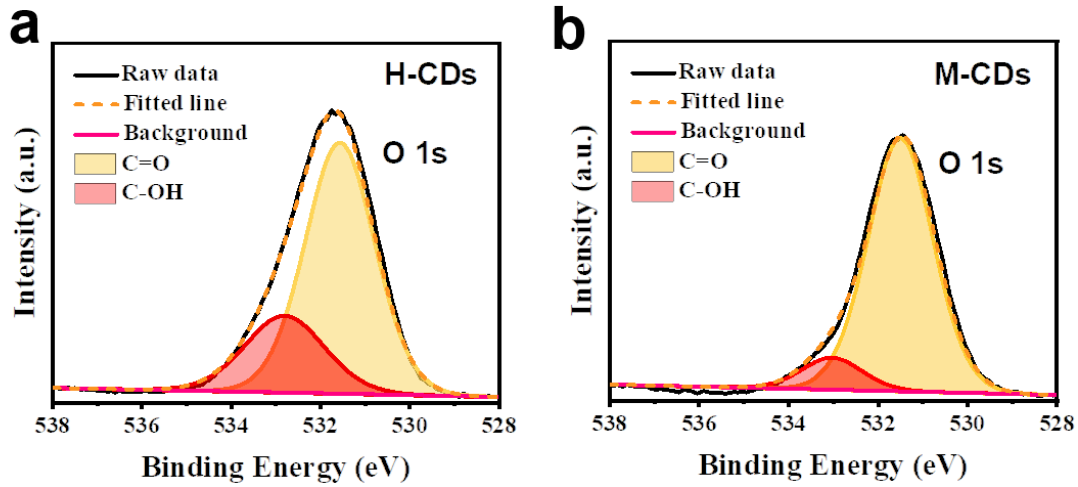


**Fig. S4** High-resolution XPS O1s spectra of (a) H-CDs and (b) M-CDs.

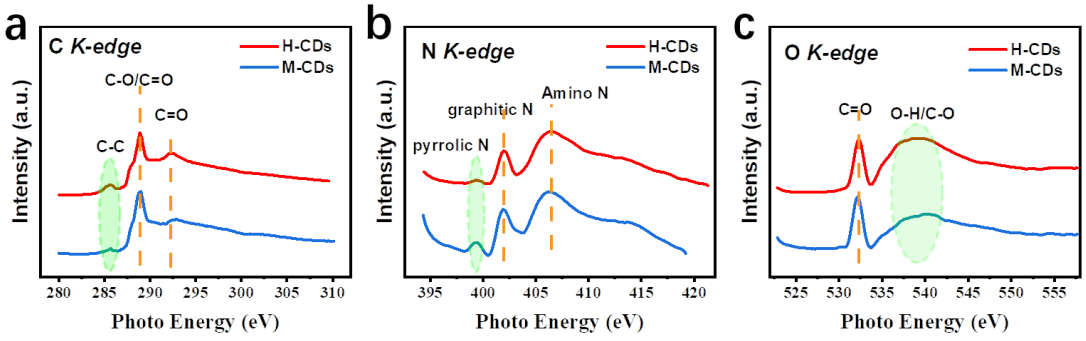


**Fig. S5** The NEXAFS spectra at the (a) C *K-edge*, (b) N *K-edge* and (c) O *K-edge* of H-CDs and M-CDs.

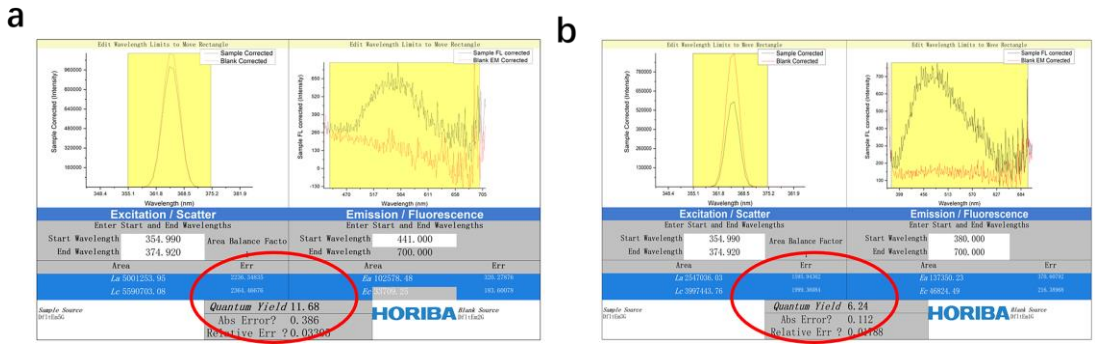


**Fig. S6** Absolute fluorescence quantum yields of (a) H-CDs and (b) M-CDs in aqueous solution.

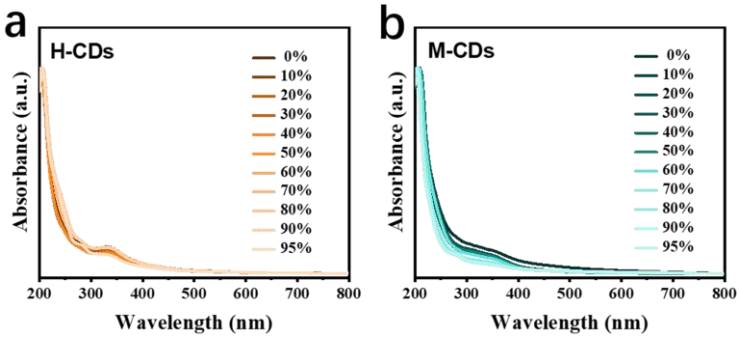


**Fig. S7** UV-Vis absorption spectra of (a) H-CDs and (b) M-CDs in the Ethanol/$H_2O$ mixtures with varying volume ratios ($f_{ethanol}$ = 0 ~ 95%).

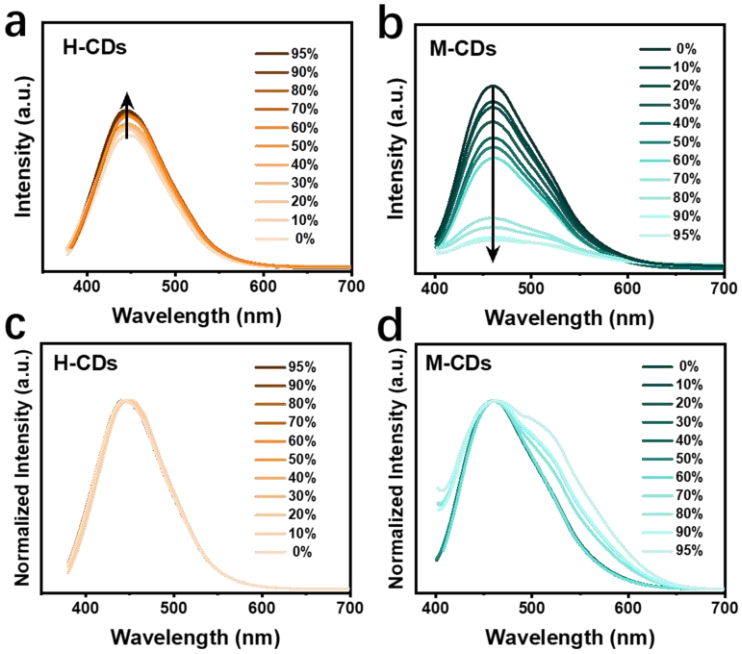


**Fig. S8** PL emission spectra of (a) H-CDs and (b) M-CDs in the Ethanol/$H_2O$ mixtures with varying volume ratios ($f_{ethanol}$ = 0 ~ 95%). Normalized PL emission spectra of (c) H-CDs and (d) M-CDs in the Ethanol/$H_2O$ mixtures.

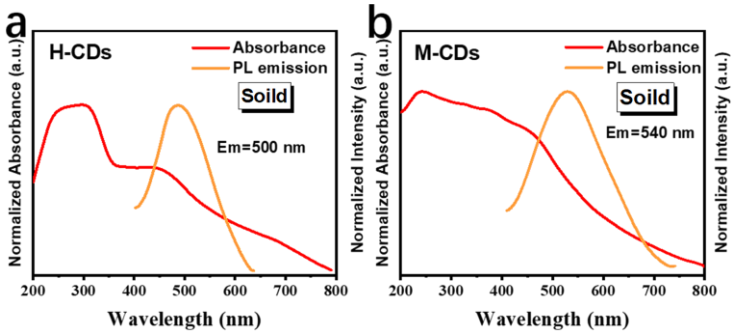


**Fig. S9** UV-vis absorption and PL spectra of (a) H-CDs and (b) M-CDs samples in solid-state.

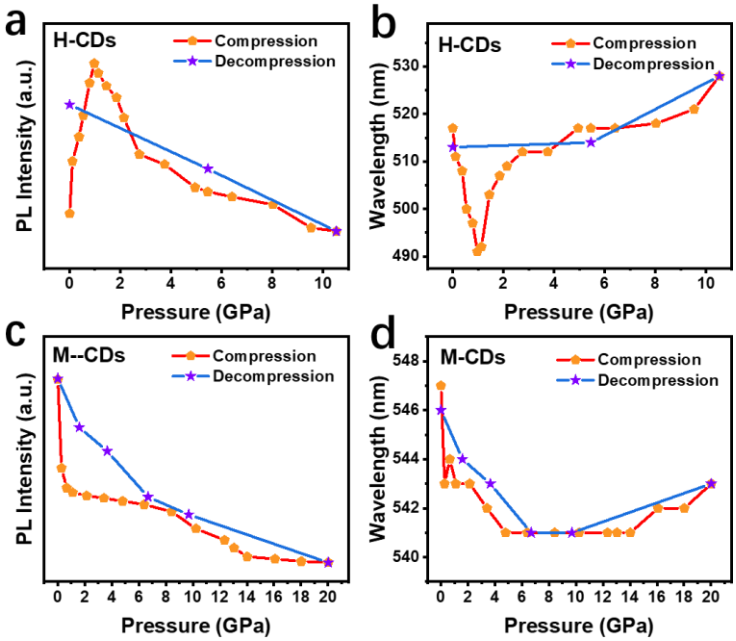


**Fig. S10** PL emission (a) intensity and (b) wavelength variations of H-CDs in the cycle of loading/unloading pressure. PL emission (c) intensity and (d) wavelength variations of M-CDs in the cycle of loading/unloading pressure.

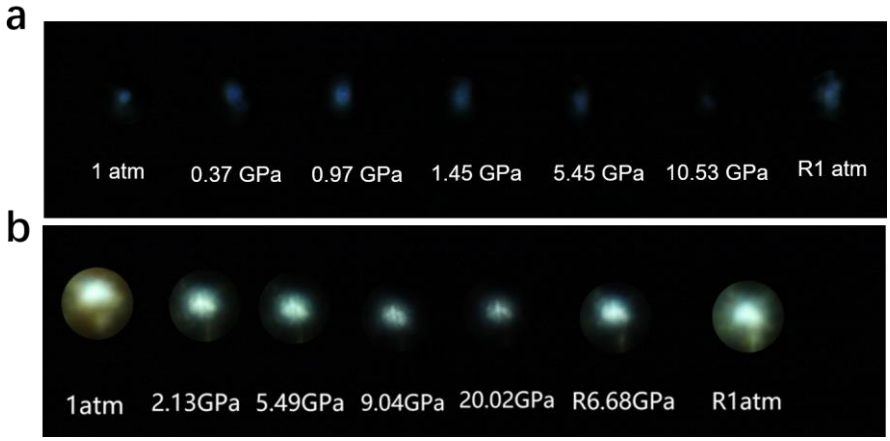


**Fig. S11** Photographs of fluorescence changes of (a) H-CDs and (b) M-CDs during loading and unloading pressure.

**Table S1** Carbon bonding composition ratio determined from the C 1s XPS of the H-CDs and M-CDs.

| Sample | C=C | C-C | C-O/C-N | C=O |
|---|---|---|---|---|
| H-CDs | 18.7 | 29.0 | 26.8 | 25.5 |
| M-CDs | 32.2 | 19.8 | 18.1 | 29.9 |

**Table S2** Nitrogen bonding composition ratio determined from the N 1s XPS of the H-CDs and M-CDs.

| Sample | Pyridinic-N | Pyrrolic-N | Graphitic-N | Amino-N |
|---|---|---|---|---|
| H-CDs | 34.7 | 35.9 | 17.1 | 11.3 |
| M-CDs | 19.4 | 47.4 | 20.3 | 12.9 |

**Table S3** Oxygen bonding composition ratio determined from the O 1s XPS of the H-CDs and M-CDs.

| Sample | C=O | C-O |
|---|---|---|
| H-CDs | 67.7 | 32.3 |
| M-CDs | 80.6 | 19.4 |